McKay, R.M., De Santis, L., Kulhanek, D.K., and the Expedition 374 Scientists
Proceedings of the International Ocean Discovery Program Volume 374
publications.iodp.org

Data report: petrology of gravel-sized clasts from Site U1521 core, IODP Expedition 374, Ross Sea West Antarctic Ice Sheet History[1]

L. Zurli,[2] M. Perotti,[2] and F.M. Talarico[2]

[1] Zurli, L., Perotti, M., and Talarico, F.M., 2022. Data report: petrology of gravel-sized clasts from Site U1521 core, IODP Expedition 374, Ross Sea West Antarctic Sheet History. *In* McKay, R.M., De Santis, L., Kulhanek, D.K., and the Expedition 374 Scientists, *Ross Sea West Antarctic Ice Sheet History*. Proceedings of the International Ocean Discovery Program, 374: College Station, TX (International Ocean Discovery Program). https://doi.org/10.14379/iodp.proc.374.201.2022

[2] Department of Physical, Earth and Environmental Sciences, University of Siena, Italy. Correspondence author: **matteo.perotti@unisi.it**

Contents

Keywords
International Ocean Discovery Program, IODP, *JOIDES Resolution*, Expedition 374, Ross Sea West Antarctic Ice Sheet History, Site U1521, Miocene, Pliocene, glaciomarine sediments, subglacial sediments, ice-rafted debris, gravel-sized clast distribution, clast petrology, mineral chemistry

Supplementary material

References (RIS)

MS 374-201
Received 17 May 2021
Accepted 24 September 2021
Published 15 February 2022

Abstract

International Ocean Discovery Program (IODP) Expedition 374 recovered high-quality cores at five sites on the Ross Sea continental shelf, slope, and rise to improve the understanding of the sensitivity of the Antarctic ice sheets (and particularly the West Antarctic Ice Sheet) to past climatic and oceanic conditions, especially during a warmer-than-present climate. This report summarizes the petrology of gravel-sized clasts from Site U1521, which is located in the Pennell Basin. The recovered core spans from the early Miocene to the Pleistocene, and it is constituted by cycles of glaciomarine sediments that indicate different paleoenvironmental conditions. Granule- to cobble-sized clasts present in the sedimentary sequence have been counted and grouped into seven different lithologies based on macroscopic and microscopic recognition. The most common lithologic group is represented by low-grade metasedimentary rocks such as metasandstone, metasiltstone, and metagraywacke. Granitoid rocks (mainly monzogranite to granodiorite) are the second most represented group. Dolerites and volcanic rocks are less frequent and are abundant only in some lithostratigraphic units. Chemical analysis of biotite from seven selected metamorphic and intrusive pebbles are also provided.

1. Introduction

International Ocean Discovery Program (IODP) Expedition 374 (January–March 2018) recovered cores from five sites along a latitudinal and depth transect from the continental shelf to the rise in the central Ross Sea (Figure **F1**) to investigate the sensitivity of the West Antarctic Ice Sheet to climatic and oceanic variations in the Neogene and Quaternary (**McKay et al.**, 2019). The principal goals of Expedition 374 were to (1) evaluate the contribution of West Antarctica to far-field ice volume and sea level estimates, (2) reconstruct ice-proximal oceanic and atmospheric temperatures to quantify past polar amplification, (3) assess the role of oceanic forcing (e.g., temperature and sea level) on Antarctic Ice Sheet (AIS) variability, (4) identify the sensitivity of the AIS to Earth's orbital configuration under a variety of climate boundary conditions, and (5) reconstruct Ross Sea paleobathymetry to examine relationships between seafloor geometry, ice sheet variability, and global climate.

Site U1521 is located in the Pennell Basin at 75°41.0351′S, 179°40.3108′W on the mid- to outer continental shelf near a northeast-southwest–oriented Miocene paleotrough (Figure **F1**) (**McKay et al.**, 2019). It consists of a single hole cored to 650.1 m drilling depth below seafloor (DSF), 411.50 m of which was recovered. Sediment is divided into seven lithostratigraphic units with different occurrences of diamictite, diatomite, diatom-rich mudstone, and mudstone as well as inter-

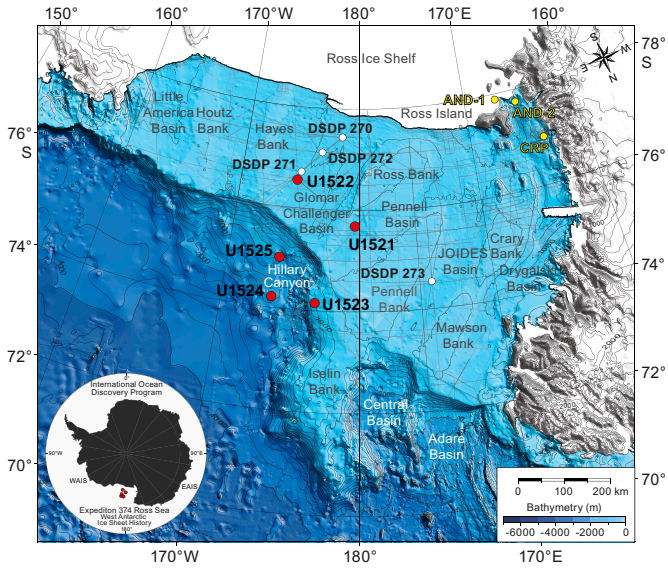

Figure F1. Bathymetric map with locations of Site U1521, other Expedition 374 sites, Deep Sea Drilling Project (DSDP) Leg 28 Sites 270–273, ANDRILL Cores AND-1 and AND-2, and Cape Roberts Project (from McKay et al., 2019).

bedded intervals of chert and conglomerate (**McKay et al.**, 2019). These sequences are interpreted to reflect different cycles of subglacial, glaciomarine, and open marine sedimentation from the early Miocene to the Pleistocene. The latter age is represented only at the top of the cored section (0–4.3 m core depth below seafloor, method A [CSF-A]) based on diatom and radiolarian biostratigraphy (**McKay et al.**, 2019). A ~15 m thick uppermost Pliocene to lower Pleistocene sequence is also present between 8.51 and 19.41 m CSF-A, whereas Pliocene sediments are separated from the underlying 500 m of middle to lower Miocene sequences (14 to <18 Ma) by a disconformity that marks a hiatus of ~11 My. The latter ages are based essentially on diatom biostratigraphy (**McKay et al.**, 2019).

In this data report, petrological analysis on clasts with a diameter >2 mm are presented following the division of the cores recovered at Site U1521 into seven lithostratigraphic units and the evaluation of the relative occurrence of lithologies recognized in the archive half sections.

Petrographic characterization of gravel-sized clasts provides a wide data set of the lithologic composition of these glaciomarine sediments. Lithology assemblages can be used to trace the changes in the mechanisms of gravel clast supply, which may be linked with the past dynamics of the Antarctic ice sheets.

2. Methods and materials

The petrology and relative abundance of clasts >2 mm were evaluated on the archive half sections of Site U1521 cores at the IODP Gulf Coast Repository at Texas A&M University (College Station, TX [USA]). Sampling, macroscopic observations, and preliminary petrographic analyses were performed following the same methods used during the Cape Roberts and Antarctic Drilling Project (ANDRILL) projects (Cape Roberts Science Team, 1998a, 1998b; Talarico and Sandroni, 1998, 2009; Talarico et al., 2000, 2012; Sandroni and Talarico, 2001). Thus, each clast >2 mm (granule to cobble granulometric fraction) was macroscopically classified into one of seven broad lithologic groups:

- Intrusive rocks with either isotropic and foliated varieties of felsic or intermediate granitoids and mafic intrusive rocks;
- Volcanic rocks with aphyric or porphyritic, vesicular, and/or amygdule-bearing varieties ranging in composition from mafic to felsic;

- Metamorphic rocks with schistose or gneissic varieties marked by mineral orientation and various low-grade metasedimentary rocks (metalimestone, metasiltstone, metasandstone, and metagraywacke);
- Sedimentary rocks with clastic lithologies (sandstone and microconglomerate with visible clastic texture) and limestone;
- Intraclasts with intrabasinal sedimentary clasts, ranging from granules to cobbles, of reworked diamictite and mud clasts;
- Dolerites with fine- to medium-grained holocrystalline, mafic subvolcanic rock with subophitic to ophitic texture; and
- Quartz grains consisting of gray vitreous single and usually monocrystalline grains.

Data processing involved counting and classifying each clast in the different lithologic groups for every 10 cm of all Site U1521 archive half cores. A total of 15,691 clasts were counted and classified. Distribution of different lithologies was then registered for each logged core except the following: Cores 374-U1521A-1R through 4R (0–31.22 m CSF-A; Lithostratigraphic Units I and II), Cores 31R–34R (285.3–315.2 m CSF-A; Lithostratigraphic Unit V), and Core 58R (515.7–524.43 m CSF-A; Lithostratigraphic Subunit VIC). Cores 10R–22R (84.2–204.95 m CSF-A; Lithostratigraphic Unit III) were logged only for the total number of clasts without any classification because they belong to mainly diatom-bearing mudstone with rare and altered clasts (**McKay et al.**, 2019). In addition, 26 clasts, mainly pebbles and cobbles, were sampled from the working half cores to produce standard petrographic thin sections for analysis by optical microscopy (Table **T1**). For each thin section, photomicrographs and a petrographic description were made (see THINSECT in **Supplementary material**). In addition, seven diamictite bulk samples were taken, dried, and sieved according to methodologies proposed by Perotti et al. (2018): the granulometric fraction >2 mm was mounted in epoxy and made into thin sections for petrographic analysis. The analysis aimed to identify grain lithologies present also in the bulk samples in which pebbles and cobbles are rare (see Table S1 in TABLES in **Supplementary material**). Classification of lithic grains followed the methods adopted in Licht et al. (2005) for metamorphic and intrusive clasts and Pompilio et al. (2007) and Panter et al. (2008) for volcanic clasts.

Seven samples, one intrusive (374-U1521A-68R-2, 58–61 cm) and six metamorphic (29R-6, 59–63 cm; 60R-5, 62–65 cm; 64R-3, 109–112 cm; 64R-6, 20–24 cm; 69R-6, 40–45 cm; and 70R-4, 120–125 cm) were selected for mineral chemistry analysis. Chemical analyses were carried out with an energy-dispersive X-ray system (Bruker Quantax 200 EDX) coupled with an electron scanning microscope (Tescan Vega3) at the Department of Physical, Earth and Environmental Sciences at the University of Siena, Italy. Analytical conditions were 20 kV accelerating voltage, 15 µA emission current, and beam spot size 0.2 µm. Natural mineral standards were used for calibration. Chemical analyses were carried out on 1 to 15 biotite crystals within each sample; crystals were selected based on the absence of alteration and/or inclusions. Cations were recalculated on the basis of 22 oxygens.

3. Results

3.1. Clast petrography

Here we present general petrological features of logged and sampled clasts from Site U1521. For a detailed description of each thin section, see THINSECT in **Supplementary material**. Figure **F2** shows photomicrographs of representative lithologies found in gravel-sized clasts.

Granitoid rocks are in general heterogranular and fine- to coarse-grained with a hypidiomorphic to allotriomorphic texture. Gray granitoids are more common than pinkish to reddish varieties. In some cases, they are isotropic granites (i.e., Samples 374-U1521A-35R-3, 65–72 cm; 55R-4, 2–5 cm; and 68R-2, 58–61 cm). In others, they show weakly foliated texture (i.e., Samples 29R-6, 59–63 cm; and 69R-6, 63–66 cm). Few samples show slightly porphyritic texture with orthoclase as the main porphyritic mineral (i.e., Samples 48R-6, 38–40 cm, and 55R-4, 2–5 cm). In general, femic

Table T1. Thin sections made from sampled clasts and bulk sediments, Site U1521. **Download table in CSV format.**

minerals are represented by biotite, which always occurs but usually is replaced by chlorite and secondary white mica. Hornblende is rarer and often chloritized (i.e., Sample 55R-4, 2–5 cm). In some cases, white mica is directly associated with biotite (i.e., Sample 29R-6, 59–63 cm). The color index ranges from 2% to 12%. Plagioclases form subhedral to euhedral laths that are in general very altered and replaced by aggregates of saussurite (sericite ± albite ± epidote ± calcite), whereas alkali feldspars (orthoclase and/or microcline) are often replaced by kaolinite and/or sericite microaggregates. Quartz is anhedral and usually interstitial with undulose extinction in some cases (i.e., Samples 29R-6, 59–63 cm, and 69R-6, 63–66 cm). One sample (64R-3, 28–31 cm) shows mortar texture with fine-grained quartz intergrowth rimming coarser crystals. Accessory phases are in general apatite, zircon/monazite, opaque minerals, and allanite. Modal compositions range from monzogranite to granodiorite.

Metamorphic rocks include metagraywackes, schists, biotite ± white mica gneisses, and phyllites. Gneiss (i.e., Sample 374-U1521A-60R-5, 62–65 cm) is heterogranular (fine to medium grained) and has granolepidoblastic texture with granoblastic domains defined by plagioclase and fine-grained quartz and biotite flakes that define the rock foliation. Another gneiss (Sample 64R-6, 20–24 cm) has lepidoblastic texture defined by iso-orientation of biotite and white mica flakes and a granoblastic domain with quartz and microcline. Schists are prevalently fine to medium grained (i.e., Samples 69R-6, 40–45 cm, and 70R-4, 120–125 cm) and have weak foliation defined by orientation of biotite and rare white mica (i.e., Samples 69R-6, 40–45 cm, and 70R-4, 120–125 cm). Phyllites (i.e., Samples 62R-4, 120–125 cm, and 63R-5, 8–17 cm) show very fine grained schistosity with lepidoblastic layers defined by biotite, opaque minerals and quartz boudins (i.e., Sample 62R-4, 120–125 cm), chlorite and quartz (i.e., Sample 63R-5, 8–17 cm), and chlorite, quartz, and opaque minerals alternations (i.e., Sample 69R-1, 120–125 cm). Metagraywackes (i.e., Samples 38R-2, 134–140 cm, and 64R-3, 109–112 cm) have very fine to medium-grained heterogranular clastic texture with biotite crystals that define weak foliation; clasts are mainly composed of quartz and minorly altered feldspar grains (plagioclase is more common than alkali feldspar) set up in an abundant argillaceous matrix and sometimes calcite cement. In general, metamorphic grade of

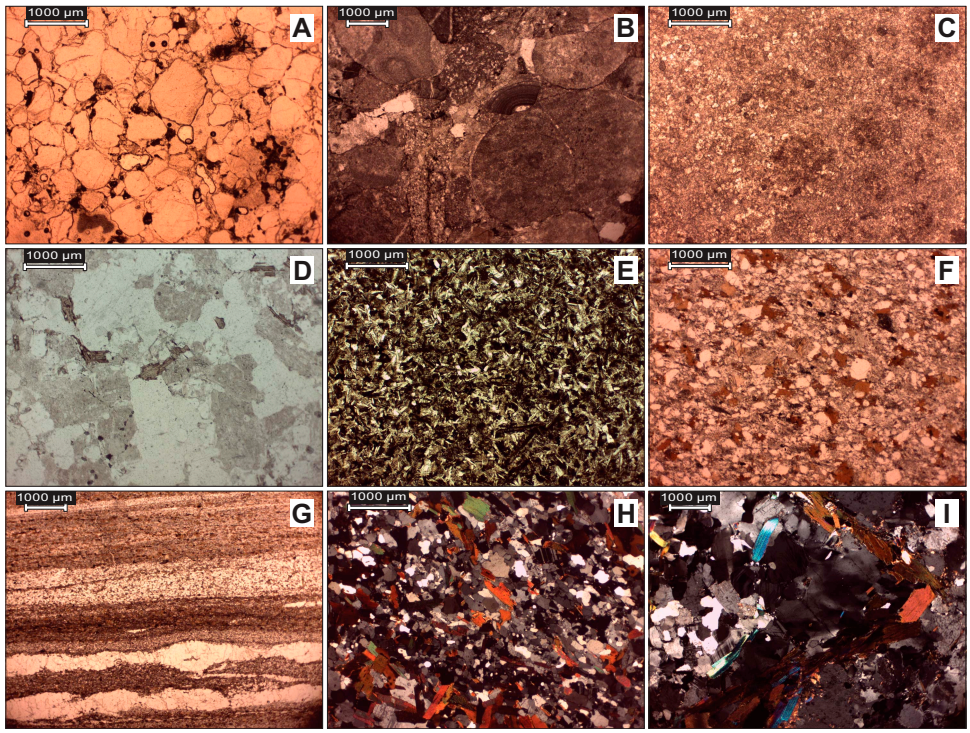

Figure F2. Photomicrographs of the main gravel-sized clast lithologies from Site U1521 core. A. Quartz-arenite, plane polarized light (PPL), magnification 2.5× (355.72 m CSF-A). B. Carbonate conglomerate, PPL, 1.6× (386.46 m CSF-A). C. Limestone, PPL, 2.5× (610.17 m CSF-A). D. Granite, PPL, 2.5× (326.27 m CSF-A). E. Basalt, PPL, 2.5× (279.34 m CSF-A). F. Biotite metagraywacke, PPL, 2.5× (577.18 m CSF-A). G. Phyllite with quartz boudins, PPL, 1.6× (559.14 m CSF-A). H. Biotite schist, cross polarized light (XPL), 2.5× (636.10 m CSF-A). I. Biotite ± white mica gneiss, XPL, 1.6× (579.95 m CSF-A).

sampled clasts is low, with paragenesis typical of greenschists/subgreenschists facies. Only in a few cases (i.e., Samples 64R-6, 20–24 cm; 69R-6, 40–45 cm; and 70R-4, 120–125 cm) does mineral paragenesis point to a medium grade.

Sampled sedimentary rocks are mudstone, siltstone, sandstone, graywacke, and limestone. Siltstone (i.e., Sample 374-U1521A-63R-CC, 10–13 cm) has mainly quartzofeldspathic silt-sized grains with isotropic texture. Sandstones are laminated mature quartz arenites composed of subrounded to well-rounded quartz grains, usually with quartz overgrowth, and minor slightly altered feldspars (i.e., Sample 38R-3, 24–28 cm) and an isotropic heterogranular (medium- to very coarse grained) matrix-rich arkosic sandstone composed of monocrystalline and polycrystalline quartz and feldspar grains (i.e., Sample 71R-1, 87–90 cm). Carbonate rocks comprise heterogranular micrite to microsparites (i.e., Samples 37R-3, 110–113 cm; 66R-4, 63–67 cm; and 67R-6, 115–120 cm) and a clast-supported coarse-grained conglomerate with clasts made of sparitic limestone, oolitic limestone, heterogranular quartz-bearing metalimestone, quartzite, and metasandstone (i.e., Sample 44R-4, 85–88 cm). Graywacke (i.e., Sample 60R-7, 90–93 cm) is composed of heterogranular (fine- to medium-grained) angular to subangular clasts made of monocrystalline quartz, minor feldspars, and felsic subvolcanic rock lithic grains.

Volcanic and subvolcanic rocks are represented by one sample (374-U1521A-30R-3, 85–89 cm) of altered basalt with holocrystalline, very fine grained subophitic texture made of plagioclase and clinopyroxene with minor interstitial quartz.

3.2. Mineral chemistry

A total of 73 chemical analyses were carried out on 7 clasts. Analyzed biotite crystals do not have any intracrystalline chemical variability; biotite representative compositions are shown in Table **T2**. A full data set of analysis is provided in TABLES in **Supplementary material**.

Figure **F3** shows biotite composition in terms of X_{Fe} [Fe/(Fe + Mg)] versus Al^{IV}. In the analyzed biotites, Al^{IV} ranges between 2.28 and 2.72 atoms per formula unit (apfu), whereas X_{Fe} ranges between 0.40 and 0.66. In each sample, analyzed biotites usually show a small compositional range. Two main compositional groups can be identified: (1) the first has X_{Fe} between 0.40 and 0.52 and Al^{IV} that varies between 2.31 and 2.58 apfu (Samples 374-U1521A-29R-6, 59–63 cm; 64R-3, 109–112 cm; 69R-6, 40–45 cm; and 70R-4, 120–125 cm). (2) The second group (Samples 60R-5, 62–65 cm; 64R-6, 20–24 cm; and 68R-2, 58–61 cm) has X_{Fe} that ranges between 0.57 and 0.66, and Al^{IV} varies from 2.28 to 2.72 apfu.

3.3. Clasts distribution

Figure **F4** shows the total number of clasts per meter along the Site U1521 core, which highlights variations in clast content and composition by lithostratigraphic unit.

Table T2. Representative composition of biotite crystals from Site U1521 clasts. **Download table in CSV format.**

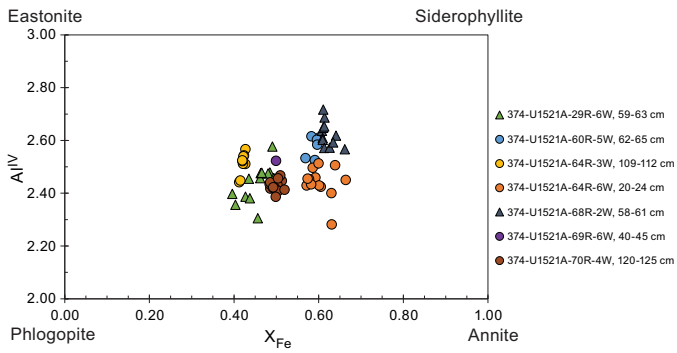

Figure F3. Biotite composition in terms of Al^{IV} versus X_{Fe} [Fe/(Fe + Mg)] for Site U1521 clasts. Compositional end-members are shown at the edges of the diagram.

Lithostratigraphic Unit II (7.4–85.34 m CSF-A) is characterized by interbedded lithified clast-poor diamictite, diatomite, and mudstone (**McKay et al.**, 2019), but recovery is very low (25%). The number of clasts varies between 0 and 30 per meter. Within this unit, clast lithologies are dominated by granitoid rocks and metamorphic rocks (on average 30.3% and 33.9% of the total amount of counted clasts, respectively). Dolerites are widely represented (16.7%), whereas other groups are present in minor amounts: quartz fragments (9.9%), volcanic rocks (5.2%), mud intraclasts (3.7%), and sedimentary rocks (0.4%).

Lithostratigraphic Unit III (85.34–209.17 m CSF-A) is a bioturbated diatom-bearing/rich mudstone sequence (**McKay et al.**, 2019). This lithostratigraphic unit is characterized by the near

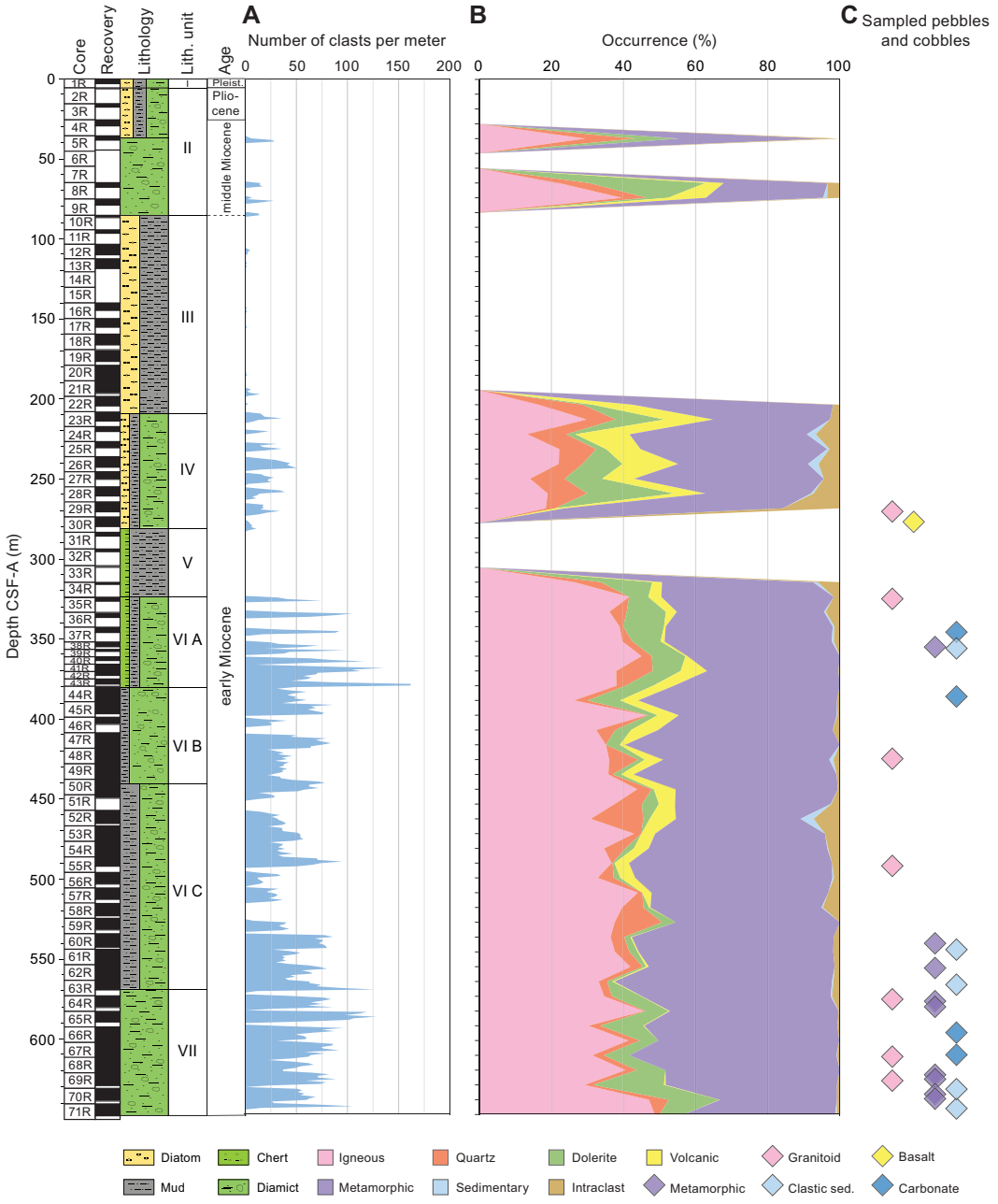

Figure F4. Site U1521 stratigraphic log (from McKay et al., 2019). A. Number of clasts per meter. B. Occurrence in percentage of each lithologic group all along the core. Percentage is calculated for each logged core; squares in the legend identify rock lithologies (modified after Marschalek et al., 2021). C. Position of sampled pebbles and cobbles and classification on the basis of thin section analysis (diamonds). See THINSECT in Supplementary material for detailed petrographic descriptions and mineral assemblage.

absence of pebbles and cobbles; the number of gravel-size clasts ranges from 0 to 10 per meter in most of the logged cores (Cores 374-U1521A-10R through 22R) (Figure **F4A**). In Lithostratigraphic Unit III, clasts were counted but not classified because they are very rare, altered, and too small to be accurately classified.

Lithostratigraphic Unit IV (209.17–280.72 m CSF-A) is diatom-bearing sandy diamictite (**McKay et al.**, 2019), and clast numbers range from 20 to 60 per meter. Clast assemblage is characterized by a high number of metamorphic rocks (45.9% on average), and granitoids are the second most abundant lithology (19.4%). Other groups represented are volcanic rock (10.6%), quartz fragments (8.9%), dolerite (8.4%), mud intraclasts (5.9%), and sedimentary rock (0.9%). The amount of metamorphic and intrusive rocks is homogeneous throughout this unit; on the other hand, dolerite clasts increase downcore, whereas volcanic rocks decrease (Figure **F4**).

Lithostratigraphic Unit V (280.72–324.20 m CSF-A) was not logged because of poor recovery (16%), drilling disturbance, and its composition of mainly chert nodules and silica-cemented mudstone lacking gravel-sized clasts (**McKay et al.**, 2019).

Lithostratigraphic Unit VI was divided into three subunits (**McKay et al.**, 2019), which are described separately.

Lithostratigraphic Subunit VIA (324.20–380.04 m CSF-A) is an interbedded sequence of clast-rich to clast-poor diamictite and mudstone (**McKay et al.**, 2019). The number of clasts is generally high, but wide variations occur along the subunit with intervals with 20 clasts per meter (i.e., Section 374-U1521A-38R-1) and intervals with as many as 160 clasts per meter (i.e., Sections 43R-2 and 43R-3). Clast lithology distribution also varies along the subunit. Granitoid rocks range from 26.3% to 45.0% of the total amount of clasts with an average value of 36.7%. Metamorphic rocks range from 36.4% to 55.2% with an average of 44.8%, and they are the most represented group. Dolerites are quite homogeneous, ranging from 5.3 to 14.2% with an average of 9.2%. Other groups are less represented (quartz fragments average 3.9%, volcanic rocks 3.3%, mud intraclasts 1.8%, and sedimentary clasts 0.3%). Six of the bulk samples from diamictites are from this unit (see Table **T1** for sample position): percentages of counted lithic grains >2 mm from analyzed thin sections are shown in Table S1 in TABLES in **Supplementary material**. Overall, percentage composition of gravel-sized lithics counted in thin sections mostly reflects that of clasts logged macroscopically. Indeed, metamorphic lithics (gneisses, schists, phyllites, metasandstones, and marbles) are the dominant group, ranging from 41% to 50% in the six analyzed samples, followed by granitoid rocks (ranging from 8% to 23%) and dolerites (ranging from 10% to 23%). Sedimentary lithic fragments are present in minor numbers, but microscopic analysis allowed scientists to discriminate between clastic sedimentary lithics (sandstones, siltstones, and conglomerates, ranging from 0% to 14%) and carbonate rocks (limestones, ranging from 0% to 8% of the total amount). Basaltic volcanic lithics range from 1% to 5%, whereas felsic porphyries range from 0% to 6% (Table S1 in TABLES **Supplementary material**).

Lithostratigraphic Subunit VIB (380.04–440.58 m CSF-A) consists of massive to stratified clast-poor to clast-rich diamictite (**McKay et al.**, 2019). Generally, the number of clasts is lower than in Subunit VIA, but wide variations occur, from 20 clasts per meter (i.e., Section 374-U1521A-48R-1) to 85 clasts per meter (i.e., Section 47R-4). Subunit VIB is characterized by a decreasing downcore number of dolerites (ranging from 0.6% to 4.3% and averaging 2.8%) and by an increasing downcore number of volcanic rocks, ranging from 1.5% to 7.5% (average = 4.9%). Most of the clasts are represented by metamorphic rocks (average = 49.8%) and intrusive rocks (average = 38.3%). Other groups are scarcely represented (<5%). One sample of bulk diamictite from this unit (see Table **T1**) was analyzed. Generally, clast composition of this sample (see Table S1 in TABLES in **Supplementary material**) reflects the macroscopic classification of clasts in this unit. The metamorphic rocks group is the most represented (42%), whereas others are less represented (intrusive = 11%, basalt = 3%, felsic porphyry = 9%, and clastic sedimentary = 7%). Moreover, dolerites are nearly absent (1%) and carbonate sedimentary rocks are completely absent.

In Lithostratigraphic Subunit VIC (440.58–567.95 m CSF-A), which consists of interbedded clast-poor diamictite and mudstone (**McKay et al.**, 2019), the number of clasts is generally lower than in Subunit VIA and varies between less than 10 per meter in clast-poor intervals to more than 90 per

meter in clast-rich intervals. Most of the unit is characterized by clasts ranging in number from 20 to 60 per meter. Subunit VIC is similar in composition to Subunit VIB. Metamorphic rocks are most abundant (average = 50.1%), and the intrusive rock group is the second most represented (average = 37.2%). Similar to Subunit VIB, dolerite occurrence is very low (average = 2.2%). The volcanic rock group is scarcely represented (average = 2.4%), as are the other groups (<5%). Volcanic clasts do not occur continuously along the subunit; they are quite rare in the lowermost portion of the subunit (504.2–568.8 m CSF-A; Cores 374-U1521A-57R through 63R), whereas they increase in the uppermost portion of the subunit (438.9–504.2 m CSF-A; Cores 50R–57R).

Lithostratigraphic Unit VII (567.95–648.17 m CSF-A) consists of interbedded clast-poor sandy to clast-rich muddy diamictite (**McKay et al.**, 2019) and is characterized by a generally high number of clasts, ranging from 20 per meter in clast-poor intervals up to 120 per meter in clast-rich intervals. This unit is characterized by a high abundance of metamorphic (average = 47.3%) and intrusive (average = 39.3%) rocks. In comparison with Subunits VIB and VIA, in Unit VII, dolerite amounts abruptly increase, representing, on average, 9.9% of the whole gravel fraction. The volcanic rocks group is almost absent in this unit, and the other groups are poorly represented within the clast assemblage (Figure **F4**).

4. Acknowledgments

We wish to thank IODP and the Gulf Coast Repository staff at Texas A&M University, College Station (USA) for their support and useful help during core logging and for having provided samples on the basis of our requests. We would like to acknowledge Dr. Andreas Laufer, who carefully reviewed this manuscript and provided useful advice and comments to improve it. We wish to also thank IODP Expedition 374 Science Party members and in particular Laura De Santis, Rob McKay, and Denise Kulhanek for their useful comments and the support they always provided us. This research is funded by Italian Antarctic Research Program (PNRA18-00233).

References

Cape Roberts Science Team, 1998a. Miocene strata in CRP-1, Cape Roberts Project, Antarctica. Terra Antartica, 5:63–124.

Cape Roberts Science Team, 1998b. Quaternary Strata in CRP-1, Cape Roberts Project, Antarctica. Terra Antartica, 5:31–62.

Licht, K.J., Lederer, J.R., and Swope, R.J., 2005. Provenance of LGM glacial till (sand fraction) across the Ross embayment, Antarctica. Quaternary Science Reviews, 24(12):1499–1520. **https://doi.org/10.1016/j.quascirev.2004.10.017**

Marschalek, J.W., Zurli, L., Talarico, F., van de Flierdt, T., Vermeesch, P., Carter, A., Beny, F., Bout-Roumazeilles, V., Sangiorgi, F., Hemming, S.R., Pérez, L.F., Colleoni, F., Prebble, J.G., van Peer, T.E., Perotti, M., Shevenell, A.E., Browne, I., Kulhanek, D.K., Levy, R., Harwood, D., Sullivan, N.B., Meyers, S.R., Griffith, E.M., Hillenbrand, C.D., Gasson, E., Siegert, M.J., Keisling, B., Licht, K.J., Kuhn, G., Dodd, J.P., Boshuis, C., De Santis, L., McKay, R.M., Ash, J., Beny, F., Browne, I.M., Cortese, G., De Santis, L., Dodd, J.P., Esper, O.M., Gales, J.A., Harwood, D.M., Ishino, S., Keisling, B.A., Kim, S., Kim, S., Kulhanek, D.K., Laberg, J.S., Leckie, R.M., McKay, R.M., Müller, J., Patterson, M.O., Romans, B.W., Romero, O.E., Sangiorgi, F., Seki, O., Shevenell, A.E., Singh, S.M., Cordeiro de Sousa, I.M., Sugisaki, S.T., van de Flierdt, T., van Peer, T.E., Xiao, W., Xiong, Z., and Expedition, I., 2021. A large West Antarctic Ice Sheet explains early Neogene sea-level amplitude. Nature, 600(7889):450–455. **https://doi.org/10.1038/s41586-021-04148-0**

McKay, R.M., De Santis, L., Kulhanek, D.K., Ash, J.L., Beny, F., Browne, I.M., Cortese, G., Cordeiro de Sousa, I.M., Dodd, J.P., Esper, O.M., Gales, J.A., Harwood, D.M., Ishino, S., Keisling, B.A., Kim, S., Kim, S., Laberg, J.S., Leckie, R.M., Müller, J., Patterson, M.O., Romans, B.W., Romero, O.E., Sangiorgi, F., Seki, O., Shevenell, A.E., Singh, S.M., Sugisaki, S.T., van de Flierdt, T., van Peer, T.E., Xiao, W., and Xiong, Z., 2019. Site U1521. In McKay, R.M., De Santis, L., Kulhanek, D.K., and the Expedition 374 Scientists, Ross Sea West Antarctic Ice Sheet History. Proceedings of the International Ocean Discovery Program, 374: College Station, TX (International Ocean Discovery Program). **https://doi.org/10.14379/iodp.proc.374.103.2019**

Panter, K., Talarico, F., Bassett, K., Del Carlo, P., Field, B., Frank, T., Hoffmann, S., Kuhn, G., Reichelt, L., Sandroni, S., Taviani, M., Bracciali, L., Cornamusini, G., von Eynatten, H., Rocchi, S., and the ANDRILL-SMS Science Team, 2008. Petrologic and geochemical composition of the AND-2A Core, ANDRILL Southern McMurdo Sound Project, Antarctica. Terra Antarctica, 15(1–2):147–192.

Perotti, M., Zurli, L., Sandroni, S., Cornamusini, G., and Talarico, F., 2018. Provenance of Ross Sea drift in McMurdo Sound (Antarctica) and implications for middle-Quaternary to LGM glacial transport: new evidence from petrographic data. Sedimentary Geology, 371:41–54. **https://doi.org/10.1016/j.sedgeo.2018.04.009**

Pompilio, M., Dunbar, N., Gebhardt, A.C., Helling, D., Kuhn, G., Kyle, P., McKay, R., Talarico, F., Tulaczyk, S., Vogel, S., Wilch, T., and the ANDRILL-MIS Science Team, 2007. Petrology and geochemistry of the AND-1B core, ANDRILL McMurdo Ice Shelf Project, Antarctica. Terra Antarctica, 14(3):255–288.

Sandroni, S., and Talarico, F., 2001. Petrography and provenance of basement clasts and clast variability in CRP-3 drillcore (Victoria Land Basin, Ross Sea, Antarctica). Terra Antartica, 8:449–467.

Talarico, F., and Sandroni, S., 1998. Petrography, mineral chemistry and provenance of basement clasts in the CRP-1 drillcore (Victoria Land Basin, Antarctica). Terra Antartica, 5:601–610.

Talarico, F., Sandroni, S., Fielding, C., and Atkins, C., 2000. Variability, petrography and provenance of basement clasts in core from CRP-2/2A, Victoria Land Basin, Antarctica. Terra Antarctica, 7:529–544.

Talarico, F.M., McKay, R.M., Powell, R.D., Sandroni, S., and Naish, T., 2012. Late Cenozoic oscillations of Antarctic ice sheets revealed by provenance of basement clasts and grain detrital modes in ANDRILL core AND-1B. Global and Planetary Change, 96–97:23–40. **https://doi.org/10.1016/j.gloplacha.2009.12.002**

Talarico, F.M., and Sandroni, S., 2009. Provenance signatures of the Antarctic Ice Sheets in the Ross Embayment during the late Miocene to early Pliocene: the ANDRILL AND-1B core record. Global and Planetary Change, 69(3):103–123. **https://doi.org/10.1016/j.gloplacha.2009.04.007**

Zurli, L., Perotti, M., and Talarico, F.M., 2022. Supplementary material, **https://doi.org/10.14379/iodp.proc.374.201supp.2022**. Supplement to Zurli, L., Perotti, M., and Talarico, F.M., 2022. Data report: petrology of gravel-sized clasts from Site U1521 core, IODP Expedition 374, Ross Sea West Antarctic Sheet History. In McKay, R.M., De Santis, L., Kulhanek, D.K., and the Expedition 374 Scientists, Ross Sea West Antarctic Ice Sheet History. Proceedings of the International Ocean Discovery Program, 374: College Station, TX (International Ocean Discovery Program).